OPEN ACCESS
Freely Available Online

JOURNAL OF ADVANCES IN NANOTECHNOLOGY
ISSN NO: 2689-2855

Research Article

DOI: 10.14302/issn.2689-2855.jan-19-2716

Marangoni Effect in Second Grade Forced Convective Flow of Water Based Nanofluid

Ghulam Rasool[1,*], Ting Zhang[1], Anum Shafiq[2]

[1]School of Mathematical Sciences, Zhejiang University, Hangzhou 310027, PR-China

[2]School of Mathematics and Statistics, Nanjing University of Information Science and Technology, Nanjing 210044, China

Abstract

Advances in nanotechnology especially in nanofluids comprising of a typical base fluid saturated with nano-size metallic particles with enhanced thermophysical properties is one of the hot topics in industrial as well as engineering applications of applied mathematics. This article explores the impact of Lorentz forces and Maragoni effect on second grade nanofluid forced convective flow. A two phase model is chosen to validate the nanofluid. Series solutions are achieved through HAM after transformation of PDEs into ODEs. The Brownian motion effect, Thermophoresis and the Marangoni effect are the main influencing factors for present flow model. In addition, the influence of pertinent fluid parameters such as Schmidt number, Magnetic number and Prandtl number on the velocity, temperature and concentration profiles is discussed with the help of graphs. With an enhanced Marangoni factor the hydraulic boundary layer thickness shows enhancement.

Corresponding author: Ghulam Rasool, School of Mathematical Sciences, Zhejiang University, Hangzhou 310027, PR-China, Email: grasool@zju.edu.cn

Keywords: Second grade Nanofluid; Nanoparticles; Marangoni effect; Forced convection; Magnetohydrodynamics.

Received: Mar 18, 2019 **Accepted:** Mar 28, 2019 **Published:** Apr 03, 2019

Editor: Muhammad Humayun, Huazhong University of Science and Technology, China.

Introduction

The concept of nanofluid is very simple but it has broadly improved the efficiency of fluids especially from industrial point of view. The suspension of nanoparticles in typical base fluid results in a very highly conductive fluid that certainly reduces the human effort as well as the machine heating. These suspensions can meet the cooling requirement for any type of thermal system. The foundation of nanofluid was laid by Choi [1] and later on, the concept became famous in all the related fields of fluid dynamics due to its industrial applications. Ibanez et al. [2] discussed an analytic investigation for MHD nanoliquid flow with suction/injection and radiation effects. Gorji et al. [3] involved a variable magnetic field for investigation of a squeezed nanofluid flow considering the Brinkman model. Related articles can be seen in [4-11] and references cited therein.

Surface tension as well as the gradients of temperature and concentration results in Marangoni convection appearing in fluid flow analysis. The topic is interesting due to its applications in crystal growth mechanism, beam melting and welding etc. Lin et al. [12] reported the Marangoni convection in nanoliquid flow via thermal gradient varying the magnetic effect. Surface tension is taken as a nonlinear temperature and concentration function. Aly and Ebaid [13] found exact solutions considering Marangoni effect in nanofluid flow using Laplace transformation method. Most recent articles can be seen in [14-17] and reference cited therein.

Present inspiration is covered by the following novel aspects. Firstly, to model a second grade nanofluid forced convective flow due to the Lorentz forces instigated into the fluid by induction of a variable magnetic field. Secondly, to achieve series solutions through HAM. The PDEs are transformed into ODEs using usual similarity transformations. Finally, to discuss the results through graphs with sufficient concluding remarks.

Problem Statement

We consider a second grade nanofluid forced convection due to the Lorentz forces instigated into the model by induction of an applied Magnetic field. The effect of magnetic field develops normal to the surface upon which the fluid is flowing. The Marangoni effect is utilized to apprehend the fluid flow in forward direction. The problem is considered in two dimensions such that the fluid flows along x-axis and the y-axis extends normal to the surface. There is no fluid motion along y-axis therefore, v=0 is taken. Along x-axis the fluid undergoes the Lorentz forces that are induced into the model due to the applied magnetic field neglecting the Hall effects. The interface temperature is taken as function of x as depicted in figure 1. The interface condition and velocity components can be visualized in figure 1.

Governing equations are therefore, as follows:

$$\frac{\partial u}{\partial x}+\frac{\partial v}{\partial y}=0, \qquad \ldots\ldots\ldots (1)$$

$$u\frac{\partial u}{\partial x}+v\frac{\partial u}{\partial y}=v_{fl}\frac{\partial^2 u}{\partial y^2}+\frac{\alpha_1}{\rho_{fl}}\left[\frac{\partial u}{\partial x}\frac{\partial^2 u}{\partial y^2}+u\frac{\partial}{\partial x}\left(\frac{\partial^2 u}{\partial y^2}\right)-\frac{\partial u}{\partial y}\frac{\partial}{\partial x}\left(\frac{\partial u}{\partial y}\right)+v\left(\frac{\partial^3 u}{\partial y^3}\right)\right]-\frac{B_0{}^2\sigma_l}{\rho_{fl}}u \qquad \ldots\ldots\ldots (2)$$

$$u\frac{\partial T}{\partial x}+v\frac{\partial T}{\partial y}=\alpha_{fl}\frac{\partial^2 T}{\partial y^2}+\frac{(\rho c)_{np}}{(\rho c)_{fl}}\left(D_B\frac{\partial c}{\partial y}\frac{\partial T}{\partial y}+\frac{D_T}{T_\infty}\left(\frac{\partial T}{\partial y}\right)^2\right) \qquad \ldots\ldots\ldots (3)$$

$$u\frac{\partial C}{\partial x}+v\frac{\partial C}{\partial y}=D_{Br}\frac{\partial^2 C}{\partial y^2}+\frac{D_{Th}}{T_\infty}\left(\frac{\partial T}{\partial y}\right)^2 \qquad \ldots\ldots\ldots (4)$$

with following boundary conditions,

$$u(x,\infty)\to 0,\ T(x,\infty)\to T_\infty,\ C(x,\infty)\to C_\infty,\ v(x,0)=0,\ T(x,0)=T_\infty+T_0X^2,\ C(x,0)=C_\infty+C_0X^2,$$
$$\mu\frac{\partial u}{\partial y}_{y=0}=-\frac{\partial\sigma}{\partial x}_{y=0}=\sigma_0\left(\gamma_C\frac{\partial C}{\partial x}_{y=0}+\gamma_T\frac{\partial T}{\partial x}_{y=0}\right), \qquad \ldots\ldots\ldots (5)$$

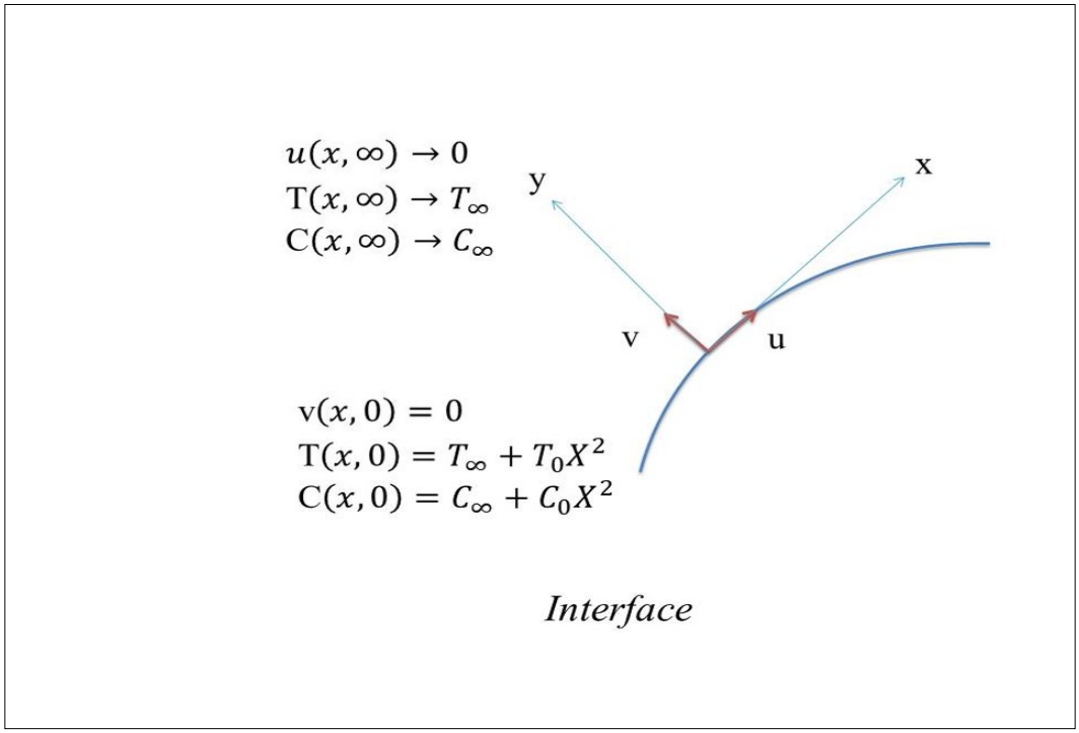

Figure 1. Schematic diagram

The surface tension, σ being a function of T and C can be defined as follows:

$$\sigma = \sigma_0[1 - \gamma_c(C - C_\infty) - \gamma_T(T - T_\infty)], \quad \text{..... (6)}$$

where

$$\gamma_C = -\frac{1}{\sigma_0}\frac{\partial\sigma}{\partial C}_T, \quad \gamma_T = -\frac{1}{\sigma_0}\frac{\partial\sigma}{\partial T}_C, \quad \text{..... (7)}$$

Here u , v are the horizontal and vertical velocity components, respectively ν_{fl} is the kinematic viscosity, ρ_{fl} is the density of fluid B_0 is the magnetic effect involved in the model for MHD, σ is the surface tension, α_{fl} is is thermal diffusivity of the fluid, the ratio between heat capacity of the nanoparticles $(\rho c)_{np}$ and heat capacity of base fluid $(\rho c)_{fl}$. D_{Br} is Brownian diffusion, D_{Th} is Thermophoresis.

Define,

$$C = C_0X^2\phi(\eta) + C_\infty, \psi = \frac{\mu}{\rho}Xf(\eta), \; T = T_0X^2\theta(\eta) + T_\infty,$$
$$\eta = \frac{y}{L}, \; v(x,y) = -\frac{\partial\psi}{\partial x}, u(x,y) = \frac{\partial\psi}{\partial y}, \quad \text{..... (8)}$$

Using (8) in

equations [1-4], we get

$$f''' + ff'' - f'^2 + \alpha(2f'f''' - f''f''' - ff^{iv}) - Mf' = 0, \quad \text{..... (9)}$$

$$\theta'' + \Pr(f\theta' - 2f'\theta) + PrN_b(\theta'\phi') + PrN_t\theta'^2 = 0, \quad \text{..... (10)}$$

$$\phi'' + \mathrm{Sc}(f\phi' - 2f'\phi) + \frac{N_t}{N_b}\theta'' = 0, \quad \text{..... (11)}$$

Subject to the Following Boundary Conditions:

$$\theta(0) = 1 = \phi(0),\ f(0) = 0,\ f''(0) = -2(1+r),$$
$$\theta(\infty) = 0 = \phi(\infty), f'(\infty) = 0\,, \qquad \text{..... (12)}$$

where $r=(C_0\ \gamma_C)/(T_0\ \gamma_T)$, $M=(L^2\ \sigma_l\ B_0)/\mu$, $Pr=\nu_{fl}/\alpha_{fl}$ is the Prandtl number $N_b=(\rho c)_{np}\ D_{B\gamma}\ C_0\ x^2) / (\rho c)_{lf}\ L^2\ a)$, $N_t=(\rho c)_{np}\ D_{Th}\ x^2) / (\rho c)_{lf}\ L^2\ a)$, $L= \mu v\ fl)/(\sigma_0\ T_0\ \gamma_T)$ are the Marangoni factor (r), modified Hartman number (M), Prandtl factor (Pr), Brownian motion parameter (Nb), Schmidt number (Sc), Thermophoresis parameter (Nt) and reference length (L), respectively. The second grade fluid parameter (α) is defined as $\alpha_1/(\rho_{fl}\ L^2)$.

Series Solutions

Homotopy analysis method [18-22] for convergent series solutions is very convenient to obtain the approximated solutions for a given nonlinear system. The method is independent of small/large physical parameters. Thus it is an efficient method as compared to other conventional methods for solving nonlinear systems. Assuming the following initial guesses,

$$f_0 = 2(1+r)(1-e^{-\eta}),\quad \theta_0 = e^{-\eta},\quad \phi_0 = e^{-\eta}. \qquad \text{..... (13)}$$

The auxiliary parameters can be defined as follows:

$$\mathrm{F}_f = \frac{\partial^3 f}{\partial \eta^3} - \frac{\partial f}{\partial \eta},\quad \mathrm{F}_\theta = \frac{\partial^2 \theta}{\partial \eta^2} - \theta,\quad \mathrm{F}_\phi = \frac{\partial^2 \phi}{\partial \eta^2} - \phi, \qquad \text{..... (14)}$$

such that,

$$\hat{\mathrm{F}}_f[M_1 e^{-\eta} + M_2 e^{\eta} + M_3] = 0,\quad \hat{\mathrm{F}}_\theta[M_4 e^{-\eta} + M_5 e^{\eta}] = 0,\quad \hat{\mathrm{F}}_\phi[M_6 e^{-\eta} + M_7 e^{\eta}] = 0, \qquad \text{..... (15)}$$

where Mi are constants for i=1-7. Subsequently, the zeroth order problems of deformation are written as follows:

$$\frac{1-p}{p\hat{h}_f}\mathrm{F}_f[\hat{f}(\eta,p) - f_0(\eta)] = N_f[\hat{f}],$$
$$\frac{1-p}{p\hat{h}_\theta}\mathrm{F}_\theta[\hat{\theta}(\eta,p) - \theta_0(\eta)] = N_\theta[\hat{f},\hat{\theta},\hat{\phi}],$$
$$\frac{1-p}{p\hat{h}_\phi}\mathrm{F}_\phi[\hat{\phi}(\eta,p) - \phi_0(\eta)] = N_\phi[\hat{f},\hat{\theta},\hat{\phi}], \qquad \text{.....(16)}$$

with following boundary conditions:

$$\hat{\theta}(0,p) = 1,\ \hat{\phi}(0,p) = 1,\ \hat{f}(0,p) = 0,\ \frac{\partial \hat{f}(0,p)}{\partial \eta^2} = -2(1+r),$$
$$\frac{\partial \hat{f}(\infty,p)}{\partial \eta} = 0,\ \hat{\theta}(\infty,p) = 0,\ \hat{\phi}(\infty,p) = 0. \qquad \text{..... (17)}$$

Therefore,

$$N_f[\hat{f}] = \frac{\partial^3 \hat{f}}{\partial \eta^3} + \hat{f}\frac{\partial^2 \hat{f}}{\partial \eta^2} - \left(\frac{\partial \hat{f}}{\partial \eta}\right)^2 + \alpha\left(2\frac{\partial \hat{f}}{\partial \eta}\frac{\partial^3 \hat{f}}{\partial \eta^3} - \frac{\partial^2 \hat{f}}{\partial \eta^2}\frac{\partial^3 \hat{f}}{\partial \eta^3} - \hat{f}\frac{\partial^4 \hat{f}}{\partial \eta^4}\right) - M\frac{\partial \hat{f}}{\partial \eta},$$
$$N_\theta[\hat{f},\hat{\theta},\hat{\phi}] = \frac{\partial^2 \hat{\theta}}{\partial \eta^2} + \mathrm{Pr}\left(\hat{f}\frac{\partial \hat{\theta}}{\partial \eta} - 2\hat{\theta}\frac{\partial \hat{f}}{\partial \eta}\right) + PrN_b\frac{\partial \hat{\theta}}{\partial \eta}\frac{\partial \hat{\phi}}{\partial \eta} + PrN_t\left(\frac{\partial \hat{\theta}}{\partial \eta}\right)^2,$$
$$N_\phi[\hat{f},\hat{\theta},\hat{\phi}] = \frac{\partial^2 \hat{\phi}}{\partial \eta^2} + Sc\left(\hat{f}\frac{\partial \hat{\phi}}{\partial \eta} - 2\frac{\partial \hat{f}}{\partial \eta}\hat{\phi}\right) + \frac{N_t}{N_b}\frac{\partial^2 \hat{\theta}}{\partial \eta^2}, \qquad \text{.....(18)}$$

where p∈ [0,1] is a typical embedding parameter and $\hat{h}_f$, $\hat{h}_\theta$, $\hat{h}_\phi$ are so-called auxiliary parameters with N_f, N_θ, N_ϕ are the non-linear operators. For p =0,1 , we have:

$$\sum_{m=0}^{\infty} f_m(\eta) = f = f_0 + \sum_{m=1}^{\infty} f_m,$$
$$\sum_{m=0}^{\infty} \theta_m(\eta) = \theta = \theta_0 + \sum_{m=1}^{\infty} \theta_m, \quad \text{..... (19)}$$
$$\sum_{m=0}^{\infty} \phi_m(\eta) = \phi = \phi_0 + \sum_{m=1}^{\infty} \phi_m$$

The m^{th} problems of deformation are

$$\mathrm{F}_f[f_m - g_m f_{m-1}] = \hat{h}_f R_f^m, \ \mathrm{F}_\theta[\theta_m - g_m \theta_{m-1}] = \hat{h}_\theta R_\theta^m, \ \mathrm{F}_\phi[\phi_m - g_m \phi_{m-1}] = \hat{h}_\phi R_\phi^m, \quad \text{..... (20)}$$

where g_m=1 for m>1 otherwise 0. Finally,

$$\Re_f^m = \frac{\partial^3 f_{m-1}}{\partial \eta^3} - \sum_{k=0}^{m-1} \frac{\partial f_{m-1-k}}{\partial \eta} \frac{\partial f_k}{\partial \eta} + \sum_{k=1}^{m-1} f_{m-1-k} \frac{\partial^2 f_k}{\partial \eta^2} +$$
$$\alpha \left(2 \sum_{k=0}^{m-1} \frac{\partial f_{m-1-k}}{\partial \eta} \frac{\partial^3 f_k}{\partial \eta^3} - \sum_{k=0}^{m-1} \frac{\partial^2 f_{m-1-k}}{\partial \eta^2} \frac{\partial^3 f_k}{\partial \eta^3} - \sum_{k=1}^{m-1} f_{m-1-k} \frac{\partial^4 f_k}{\partial \eta^4} \right) - M \frac{\partial f_m}{\partial \eta},$$
$$\Re_\theta^m = \frac{\partial^2 \theta_{m-1}}{\partial \eta^2} + \mathrm{Pr} \sum_{k=0}^{m-1} f_{m-1-k} \frac{\partial \theta_k}{\partial \eta} - 2Pr \sum_{k=0}^{m-1} \theta_{m-1-k} \frac{\partial f_k}{\partial \eta} + N_b Pr \sum_{k=0}^{m-1} \frac{\partial \theta_{m-1-k}}{\partial \eta} \frac{\partial \phi_k}{\partial \eta} + N_t Pr \sum_{k=0}^{m-1} \frac{\partial \theta_{m-1-k}}{\partial \eta} \frac{\partial \theta_k}{\partial \eta},$$
$$\Re_\phi^m = \frac{\partial^2 \phi_{m-1}}{\partial \eta^2} + Sc \sum_{k=0}^{m-1} f_{m-1-k} \frac{\partial \phi_k}{\partial \eta} - 2Sc \sum_{k=0}^{m-1} \frac{\partial f_{m-1-k}}{\partial \eta} \phi_k + \frac{N_t}{N_b} \sum_{k=0}^{m-1} \frac{\partial \theta_{m-1-k}}{\partial \eta} \frac{\partial \theta_k}{\partial \eta}. \quad \text{.....(21)}$$

Thus,

$$f_m = M_1 + M_2 e^{\eta} + M_3 e^{-\eta} + f_m^*(\eta),$$
$$\theta_m = M_4 e^{\eta} + M_5 e^{-\eta} + \theta_m^*(\eta),$$
$$\phi_m = M_6 e^{\eta} + M_7 e^{-\eta} + \phi_m^*(\eta), \quad \text{..... (22)}$$

are the general solutions where Mi are the arbitrary constants for i=1-7 and $f_m^*(\eta)$, $\theta_m^*(\eta)$, $\phi_m^*(\eta)$ are special solutions.

Convergence Analysis

The auxiliary parameters introduced in (series solution) for the velocity profile (f), temperature distribution (θ) and concentration distribution (ϕ) are termed as convergence control parameters. These parameters are significant to speed-up the convergence. Convergence intervals are sketched in Fig. 2. The interval of interest for convergence of the aforementioned profiles is [-0.60, 0.30].

Results and Discussion

This section is concerned with the discussion on graphical results that are obtained through Mathematica based HAM code for specific values of pertinent fluid parameters including the second grade fluid parameter, the Magnetic number, the Marangoni ratio, the Prandtl and Schmidt numbers as well as the Brownian and Thermophoretic parameters. Fig. 3. displays the effect of second grade fluid parameter on the velocity profile. The velocity shows decreasing behavior for incremental values of respective parameter. A certain increase in viscosity results in decrease of fluid motion. The velocity shows reduction with augmented values of Marangoni ratio as depicted in Fig. 4. Similar is the case noticed for Magnetic number as displayed in Fig. 5. A significant drop in velocity profile appears at first sight however, the variation slows down with the stronger effect of magnetic number. The temperature profile, as displayed in Fig. 6, shows augmented behavior with augmented values of Marangoni ratio. However, after certain limitation, the effect can be seen in opposite nature. The Prandtl number shows enhancement in temperature profile due to an enhanced thermal diffiusivity as one can see in Fig.7. Fig. 8 and Fig. 9 are the display of variation in Temperature profile varying the values of Brownian motion parameter and Thermophoretic parameter, respectively. The rapid and in-predictive movement of nanoparticles as well as the more stronger Thermophoretic force results in incremental behavior of temperature profile. The effect of Marangoni ratio on concentration profile is displayed in Fig. 10. The results persist with those appearing in Temperature profile for the same parameter. An opposite behavior is seen upon variation of Thermophoretic parameter and Schmidt number for concentration profile as displayed in Fig. 11 and Fig. 12, respectively.

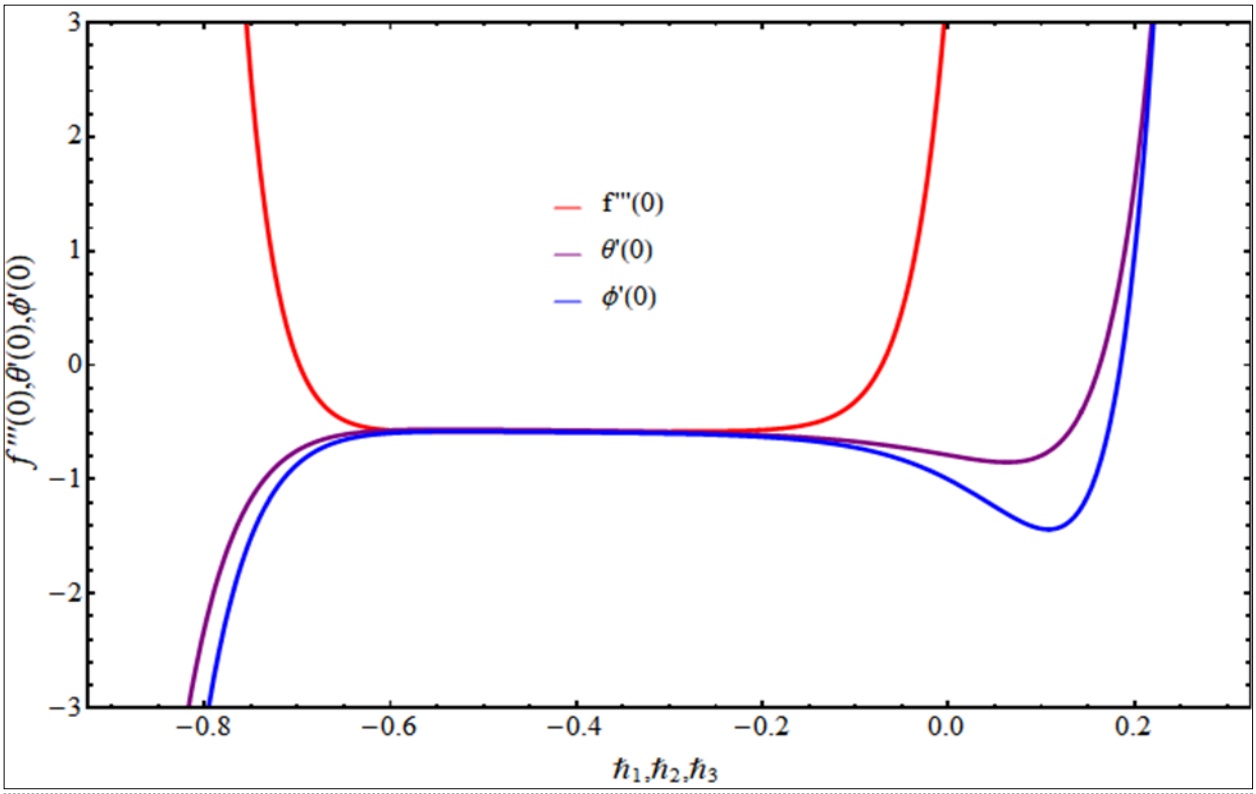

Figure 2. H-Curves for convergent series solutions

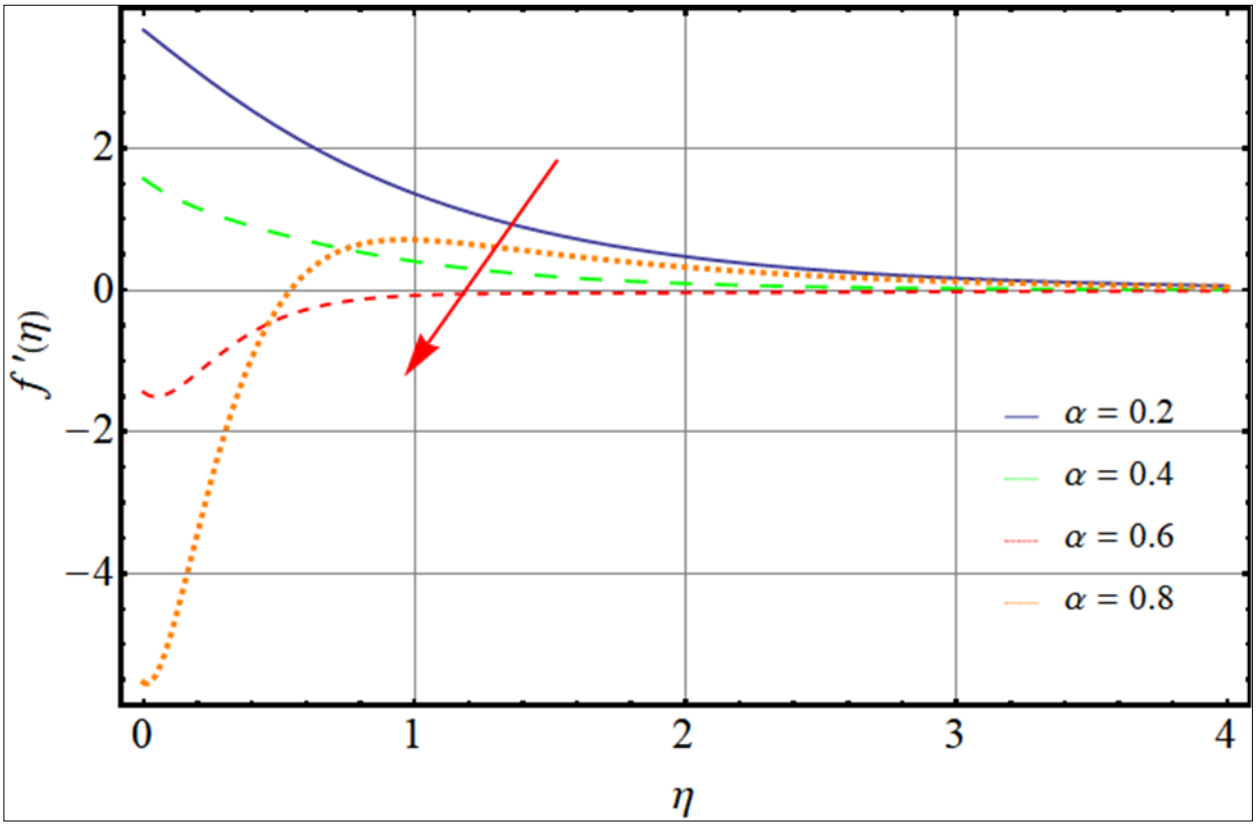

Figure 3. Impact of second grade parameter on velocity profile

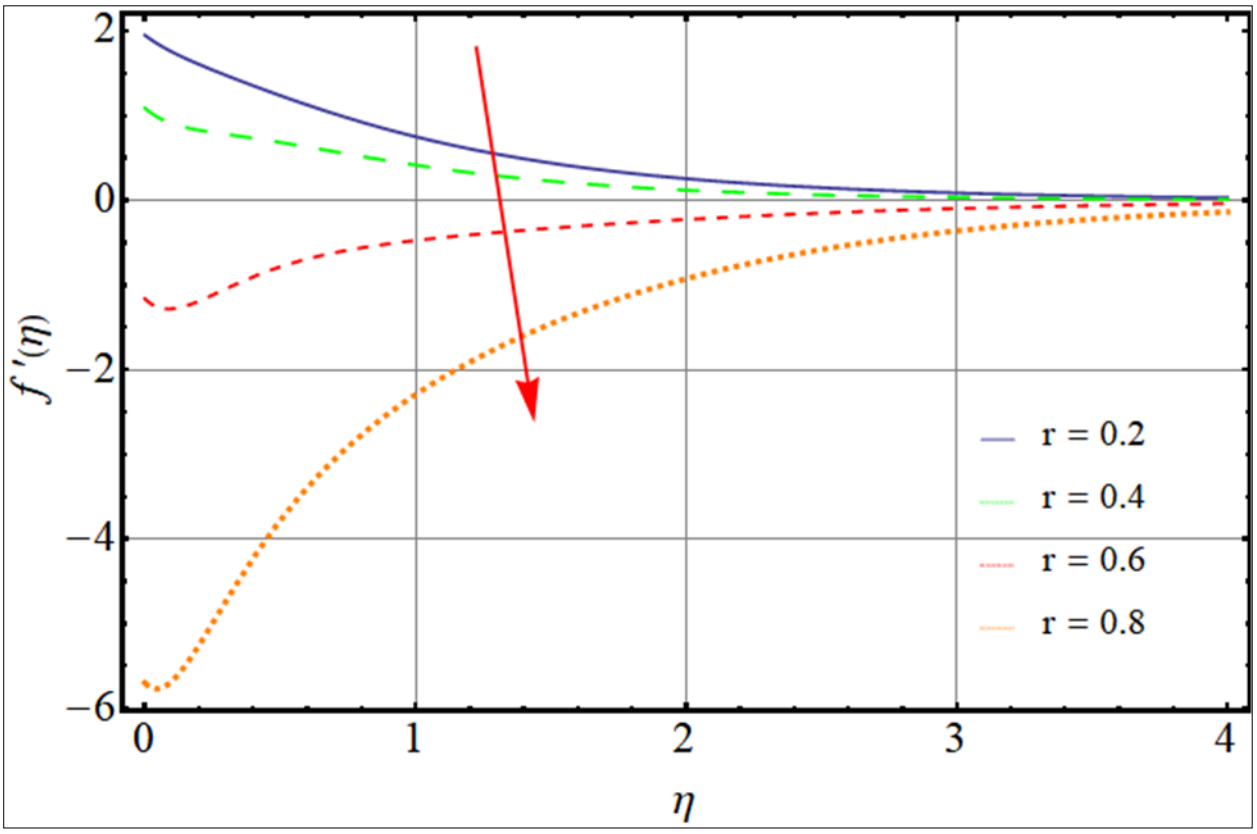

Figure 4. Impact of Marangoni ratio on velocity profile

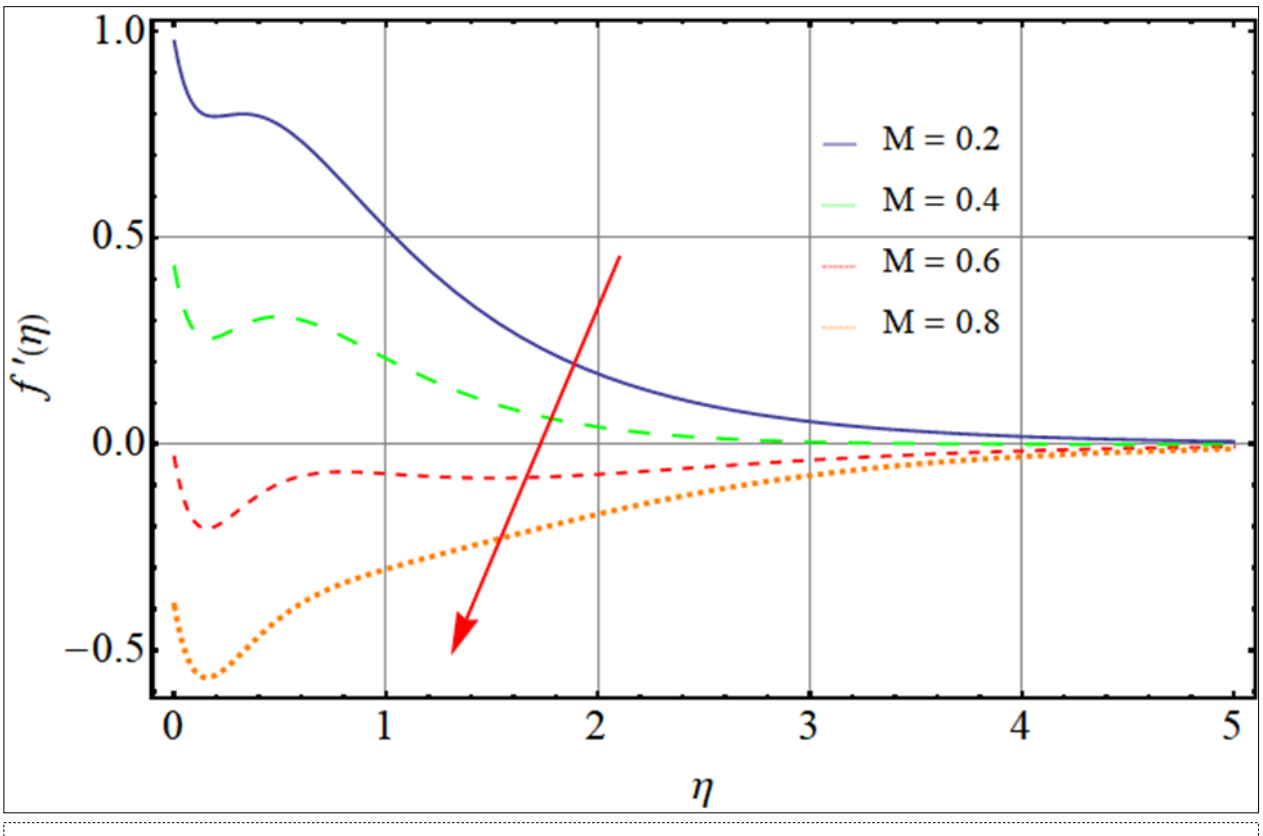

Figure 5. Impact of magnetic number on velocity profile

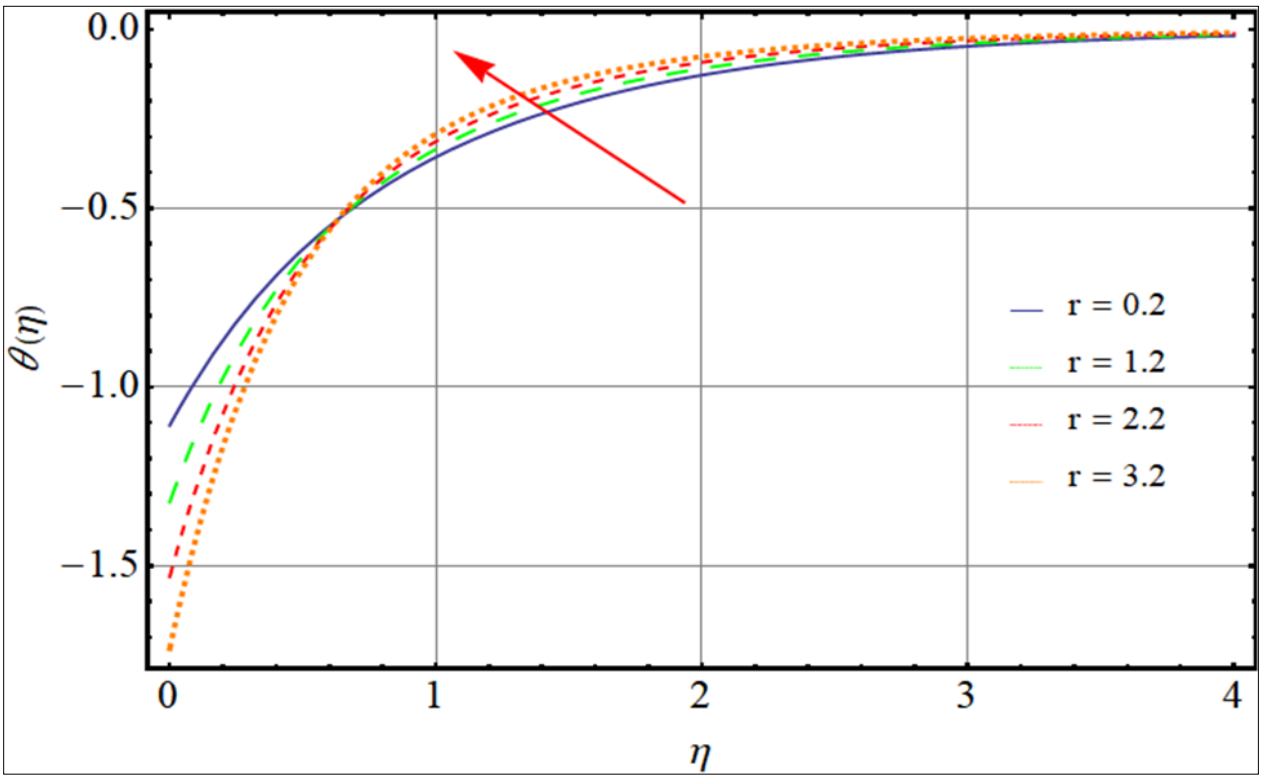

Figure 6. Impact of Marangoni ratio on temperature profile

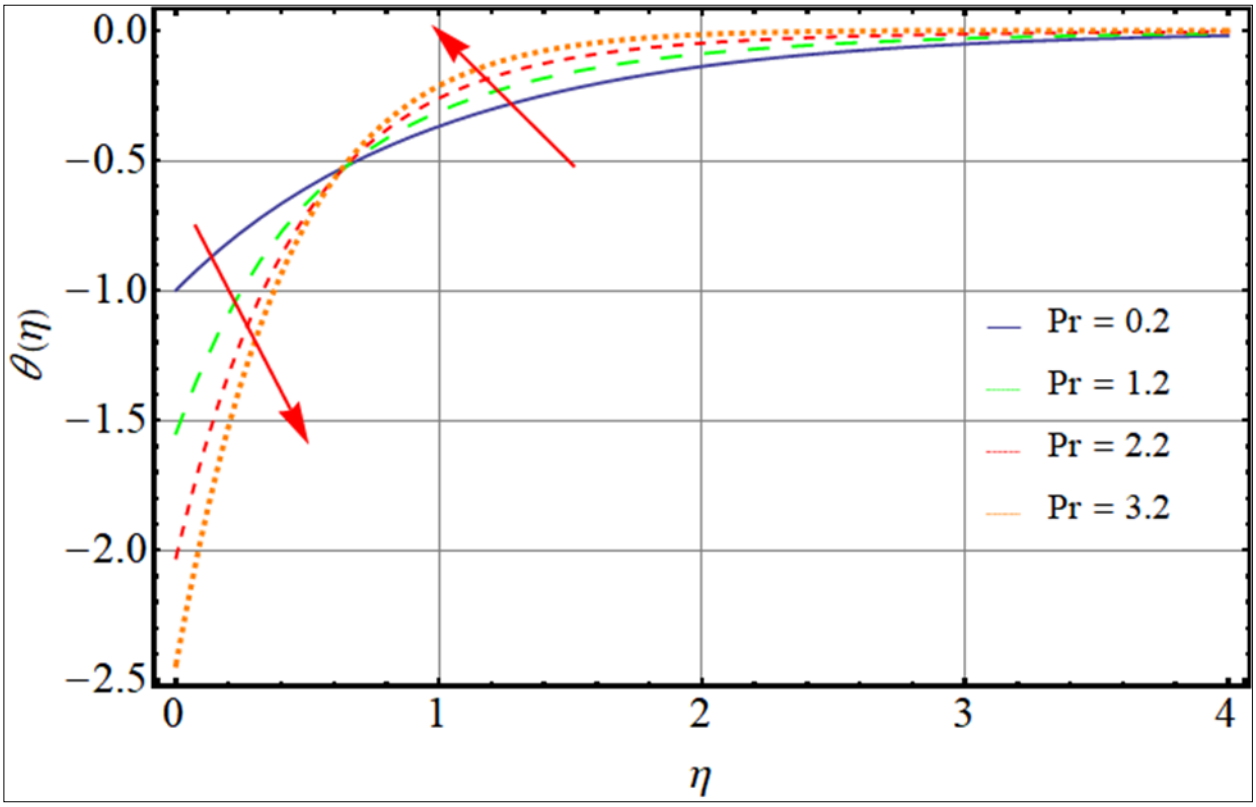

Figure 7. Impact of Prandtl number on temperature profile

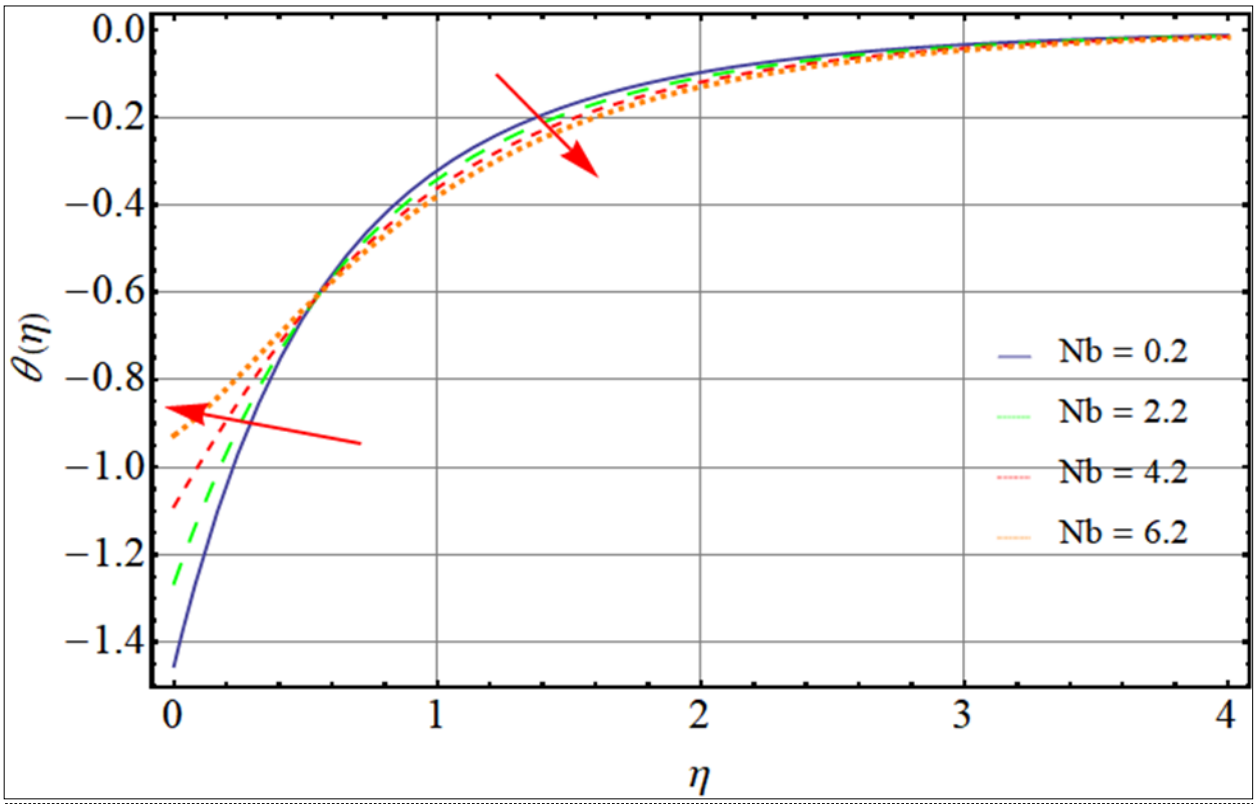

Figure 8. Impact of Brownian motion on temperature profile

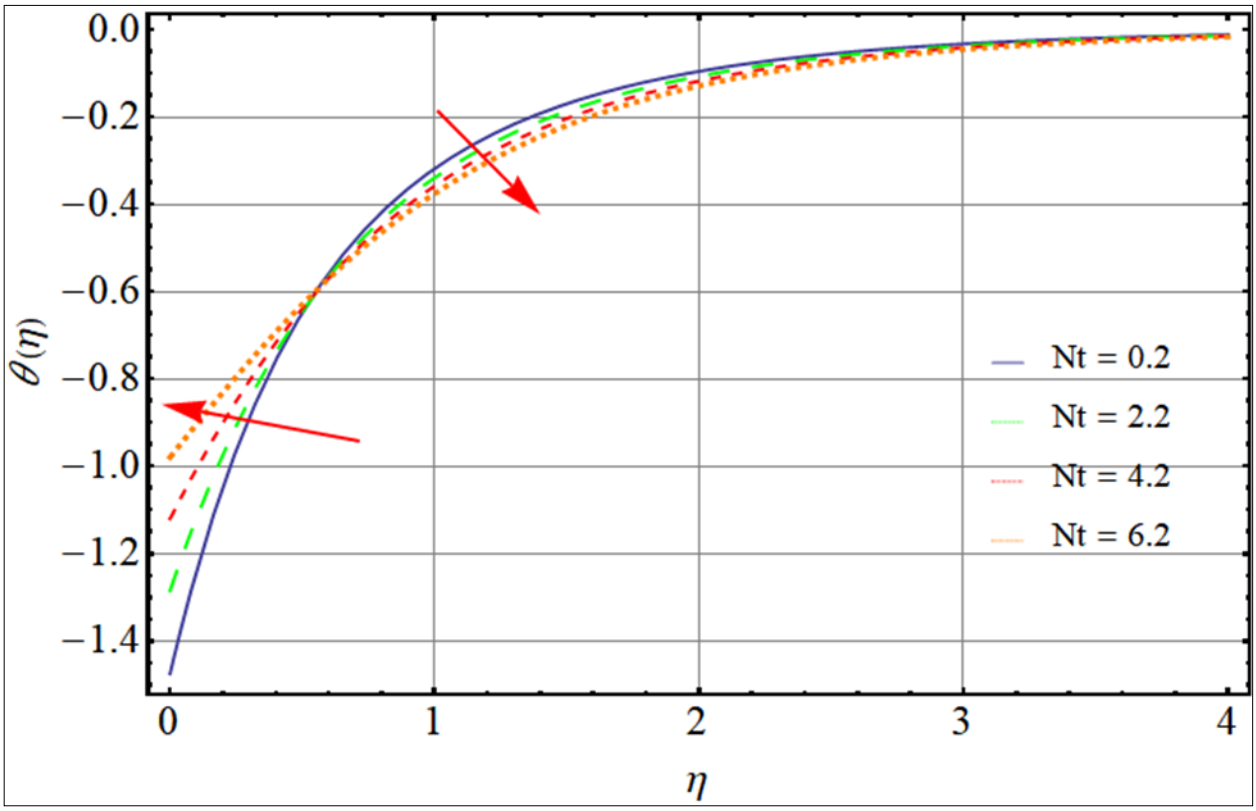

Figure 9. Impact of Thermophoresis on temperature profile

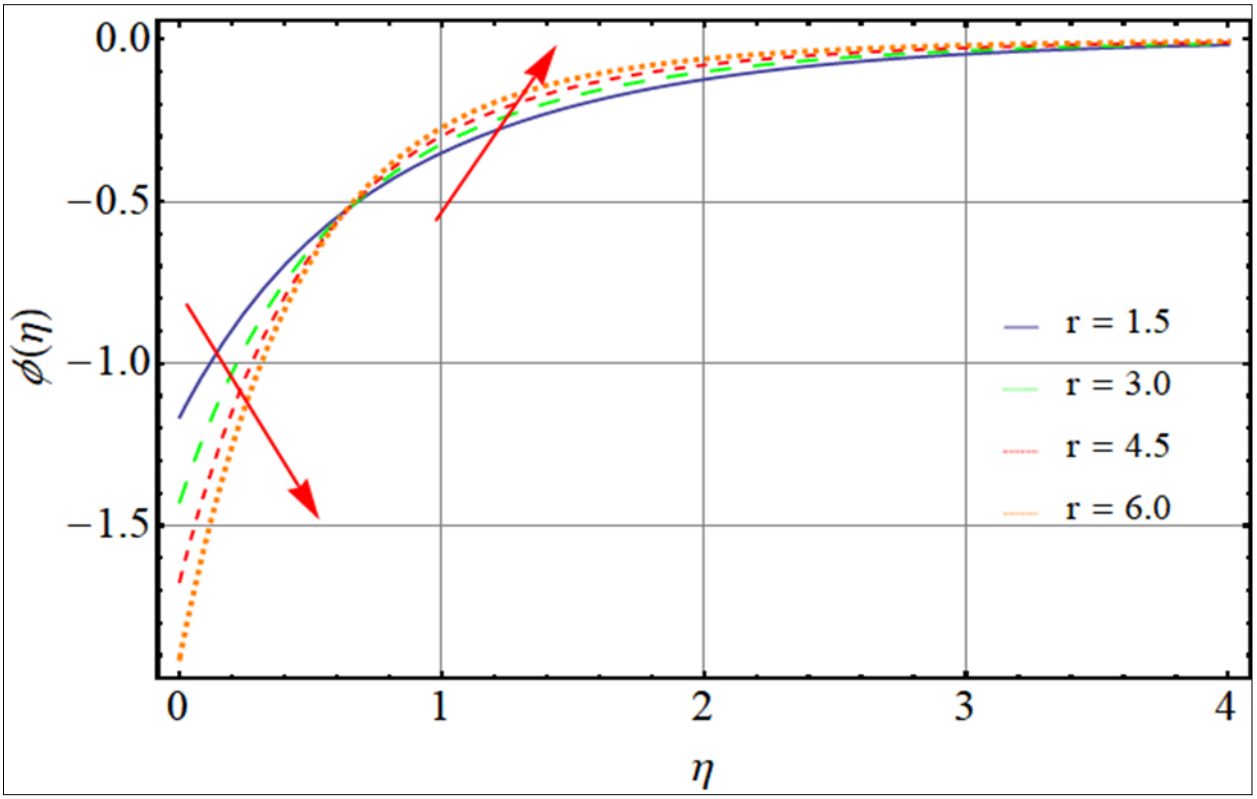

Figure 10. Impact of Marangoni ratio on concentration profile

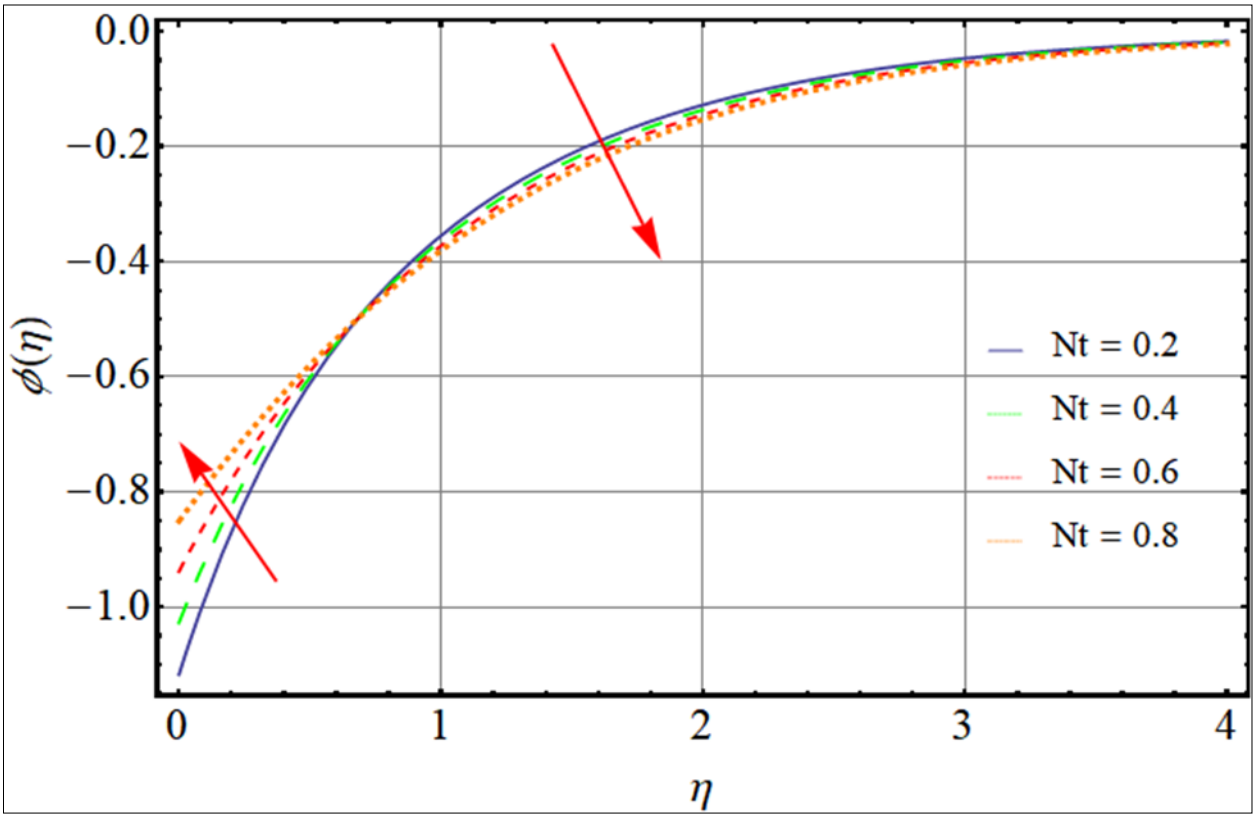

Figure 11. Impact of Thermophoresis on concentration profile

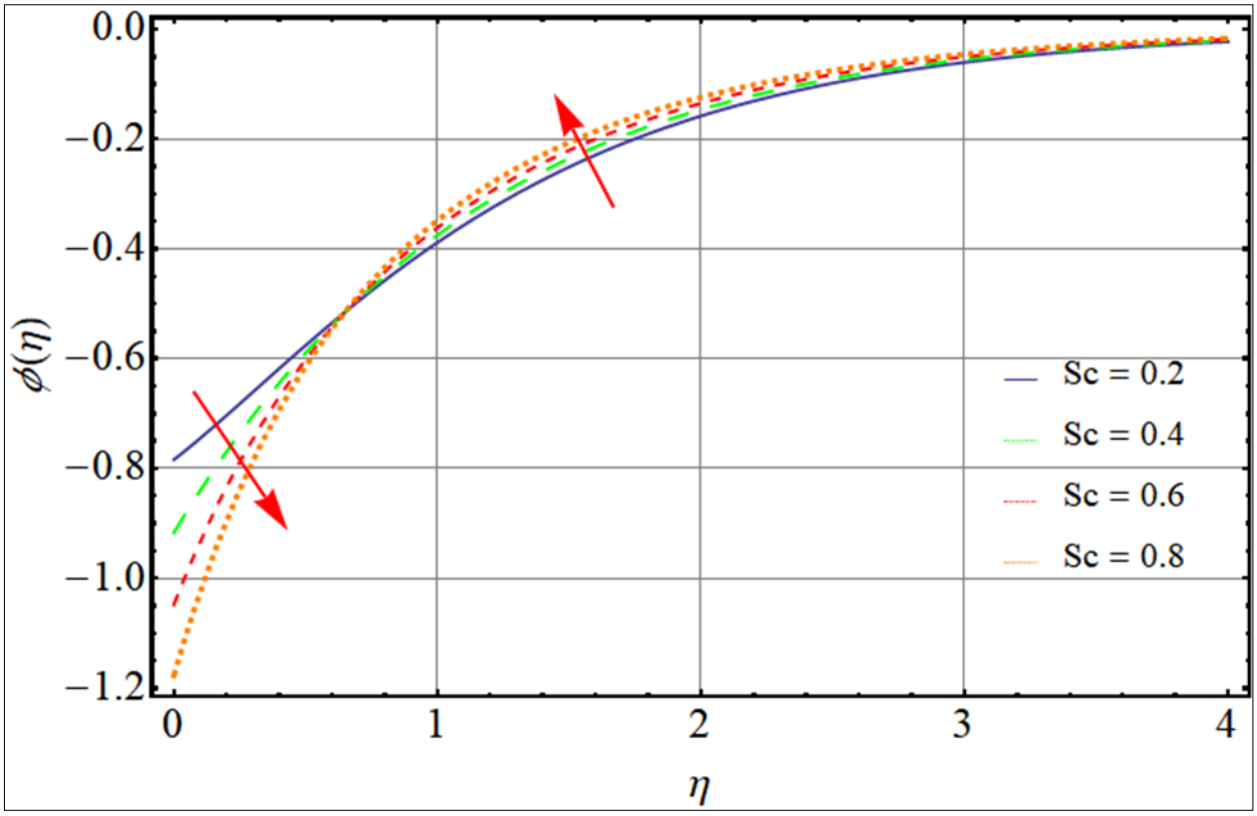

Figure 12. Impact of Schmidt number on concentration profile

Closing Remarks

This study concludes with the impact of Marangoni effect and Lorentz force generated by MHD on second grade nanofluid flow. Flow model is formulated mathematically in PDEs which are transformed into ODEs using transformation and HAM is applied to get the convergent series solutions. We conclude that velocity profile reduces for stronger Marangoni effect in second grade nanofluid. The Brownian motion and Thermophoresis have significant impact on the flow profiles. Furthermore, the temperature and concentration profile shows augmented behavior with augmented Marangoni ratio. One can see that due to strong impact of Lorentz forces, a reduction in hydraulic boundary layer is noticed however, an opposite behavior is shown the other two profiles.

References

1. S. U. S. Choi, Enhancing thermal conductivity of fluids with nanoparticles, D. App. Non-Newtonian Flows. 231 (1995) 99-105.
2. G. Ibanez, A. Lupez, J. Pantoja and J. Moreira, Entropy generation analysis of a nanofluid flow in MHD porous microchannel with hydrodynamic slip and thermal radiation. Int. J. H. M. Trans. 100 (2016) 89-97.
3. M. R. Gorji, O. Pourmehran, M. G. Bandpy and D. D. Ganji, Unsteady squeezing nanofluid simulation and investigation of its effect on important heat transfer parameters in presence of magnetic field. J. T. Inst. Chem. Eng. 67 (2016) 467-475.
4. K. L. Hsiao, To promote radiation electrical MHD activation energy thermal extrusion manufacturing system eÂ¢ ciency by using Carreau-Nanofluid with parameters control method. Energy 130 (2017) 486-499.
5. F. Mabood, W. A. Khan and A. I. M. Ismail, MHD boundary layer flow and heat transfer of nanofluids over a nonlinear stretching sheet: A numerical study. J. Mag. Mag. Mat. 374 (2015) 569-576.
6. C. S. K. Raju and N. Sandeep, Unsteady Casson nanofluid flow over a rotating cone in a rotating frame filled with ferrous nanoparticles: A Numerical study. J. Mag. Mag. Mat. 421 (2017) 216-224.

7. A. Shafiq, Z. Hammouch and T. N. Sindhu, Bioconvective MHD flow of Tangent hyperbolic nanofluid with Newtonian heating. Int. J. Mech. Sci. 133 (2017) 759-766.
8. M. Azam, M. Khan and A. S. Alshomrani, Effects of magnetic field and partial slip on unsteady axisymmetric flow of Carreau nanofluid over a radially stretching surface. Res. Phys. 7 (2017) 2671-2682.
9. F. Naseem, A. Shafiq, L. Zhao and A. Naseem, MHD biconvective Ãiow of Powell Eyring nanofluid over stretched surface. AIP Adv. 7 (2017) 065013.
10. J. V. R. Reddy, V. Sugunamma and N. Sandeep, Thermophoresis and Brownian motion effects on unsteady MHD nanofluid flow over a slendering stretching surface with slip effects. Alex. Eng. J. (2017) 065013.
11. G. C. Shit, R. Haldar and S. Mandal, Entropy generation on MHD flow and convective heat transfer in a porous medium of exponentially stretching surface saturated by nanofluids. Adv. P. Tech. 28 (2017) 1519-1530.
12. Y. Lin, L. Zheng, X. Zhang, MHD Marangoni boundary layer flow and heat transfer of pseudo-plastic nanofluids over a porous medium with a modified model, Mech Time-Depend Mater, 4 (2015) 519-36.
13. E. H. Aly, A. Ebaid,Exact analysis for the effect of heat transfer on MHD and radiation Marangoni boundary layer nanofluid flow past a surface embedded in a porous medium, J Mol Liquids, 215 (2016) 625-39.
14. N. A. A. Mat, N. M. Arifin, R. Nazar, Radiation effect on Marangoni convection boundary layer flow of a nanofluid.Mathemat Sci, (2012 1(6) 1-6.
15. G. S. Gevorgyan, K. A. Petrosyan, R. S. Hakobyan, and R. B. Alaverdyan, Experimental Investigation of Marangoni Convection in Nanofluids, Journal of Contemporary Physics (Armenian Academy of Sciences), 4(2017) 362-365.
16. Abdullah Al-Sharafi, Z. Ahmet, Bekir Sahin, S. Yilbas and S. Z. Shuja, Marangoni convection flow and heat transfer characteristics of waterâ€"CNT nanofluid droplets, Numerical Heat Transfer, Part A: Applications, 7(2016) 763-780.
17. G. Rasool, T. Zhang, A. Shafiq, H. Durur, Influence of Chemical Reaction on Marangoni Convective Flow of Nanoliquid in the Presence of Lorentz Forces and Thermal Radiation: A Numerical Investigation. J. Adv. Nanotech. 1(2019) 32-49.
18. K. Bhattacharyya, Effects of radiation and heat source/sink on unsteady MHD boundary layer flow and heat transfer over a shrinking sheet with suction/injection, Front. Chem. Sci. Eng. 5(2011) 376--384.
19. B. Lavanya, A.L. Ratnam, Radiation and mass transfer effects on unsteady MHD natural convective flow past a vertical porous plate embedded in a porous medium in a slip flow regime with heat source/sink and Soret effect, Int. J. Eng. Tech. Res. 2 (2014) 376--384.
20. I. Ali, G. Rasool, S. Alrashed, Numerical simulations of reaction--diffusion equations modeling prey--predator interaction with delay, Int. J. Bio. 11 (2018) 1850-054.
21. A. Naseem, A. Shafiq, L. Zhao, M.U. Farooq, Analytical investigation of third grade nanofluidic flow over a riga plate using Cattaneo-Christov model Res. Phy. 9(2018) 961-969.
22. M.Khan, M.Irfan, W.A.Khan, Impact of heat source/ sink on radiative heat transfer to Maxwell nanofluid subject to revised mass flux condition, Res. Phy. 9 (2018) 851-857.